Int. J. Heat Mass Transfer. Vol. 34, No. 9, pp. 2187–2197, 1991
Printed in Great Britain

0017-9310/91 $3.00+0.00
Pergamon Press plc

Heat transfer and friction characteristics of spirally corrugated tubes for power plant condensers—1. Experimental investigation and performance evaluation

V. D. ZIMPAROV, N. L. VULCHANOV and L. B. DELOV
School of Mechanical and Electrical Engineering, 4, 'H. Dimitar' Str., 5300 Gabrovo, Bulgaria

(*Received* 17 *October* 1989 *and in final form* 10 *October* 1990)

Abstract—Heat transfer and isothermal friction pressure drop results are obtained experimentally for one smooth and 25 spirally corrugated brass tubes for power plant condenser applications. The height of the ridge is varied from 0.44 to 1.18 mm and the pitch of corrugation from 6.5 to 16.9 mm. The spiral angle of the ridge (with respect to the tube axis) is in the range 68–85 deg and the Reynolds number is in the range of 10^4–6×10^4. Heat transfer and pressure drop data are shown in forms convenient for easy comparison with those of other authors. They are used to predict theoretically Fanning friction factors and heat transfer enhancement at both sides of the tube via a unified mathematical model requiring at input the Reynolds and Prandtl numbers and the geometrical parameters of the ridge. Performance evaluation criteria are used to obtain quantitative estimates of the benefits offered by the spirally corrugated tubes.

INTRODUCTION

RECENTLY enhancement of heat transfer has been focused on techniques for increasing the heat transfer coefficients in different heat exchange applications. The trend is to develop more compact and cheaper heat exchangers or to increase the systems' thermodynamic efficiency while reducing the operating costs. Many augmentation techniques are reported [1, 2], each having its own merits and demerits. References [3–11] reveal that the spirally corrugated tubes provide several advantages over other rough surfaces such as finned tubes, sand-grain textures, wire-coil inserted tubes or transverse rib roughened tubes. Some of these are: (i) easier fabrication, (ii) limited fouling and (iii) higher enhancement of the heat transfer rate compared to the increase of the friction factor.

Steam condensers for desalination and power plants can be designed to utilize corrugated tubes with significant economic benefits. Until recently, however, virtually all plants utilized standard, smooth tubes for the main condenser, auxiliary turbine condensers or feed water heaters. Although the spirally corrugated tubes are commercially available [5, 12], limited experimental investigations of their behaviour in power plant condensers have been conducted [13, 14]. Complete retubing was reported in ref. [15].

The lack of a systematic study on single and multistart spirally corrugated tubes for condensation/convective heat transfer applications hinders the prediction of optimal tube geometry and general correlations are not available. Many authors have analysed the results for the friction factors in single- and multistart spirally corrugated tubes in terms of the momentum transfer roughness function R, defined from

$$R(e^+) = (2/f)^{0.5}+2.5\ln(2e/D_i)+3.75 \qquad (1)$$

which was correlated by either the roughness Reynolds number e^+, the Reynolds number Re, and the geometrical parameters p/e and β_* [8, 10, 11], or the group $e^2/(pD_i)$ termed as the tube severity factor [6, 10] and introduced in ref. [16]. Experimental heat transfer data have been analysed using the heat transfer roughness function $G(e^+, Pr)$, defined as

$$G(e^+, Pr) = \frac{(f/2St-1)}{\sqrt{(f/2)}}+R(e^+). \qquad (2)$$

Bergles *et al.* [17] proposed performance evaluation criteria (PEC) and developed a method to evaluate the performance effectiveness of existing surfaces for which St and f data were available. These methods were used in refs. [8, 10, 11] to assess the performance of particular corrugated tubes. The ratios calculated following ref. [17], however, should be interpreted as limits since the external thermal resistance was neglected and the driving temperature difference was assumed constant throughout the exchanger. The estimate [7] obtained by the extended criteria [18] seems to be more realistic. A comprehensive treatise on PEC was reported later in ref. [19] and we utilize Webb's criteria [19] in what follows.

The purpose of this study is to develop correlations to predict friction factors and heat transfer coefficients at both sides of the tube in terms of the Reynolds and Prandtl numbers and the geometrical parameters of the ridge. Further the PEC suggested by Webb [19]

NOMENCLATURE

A	heat transfer surface area [m^2]
c_p	specific heat capacity [J kg^{-1} K^{-1}]
D	tube diameter [m]
e	height of the ridge [m]
h	heat transfer coefficient [W m^{-2} K^{-1}]
k	thermal conductivity [W m^{-1} K^{-1}]
p	pitch of corrugation [m]
P	pumping power [W]
Q	heat rate [W]
R_1, R_2	radii, equation (14) [m]
s	cap height of the ridge [m]
t	cap width of the ridge [m]
T	temperature [K]
U_m	mean fluid velocity, $[4\dot{V}/(\pi D_i^2)]$ [m s^{-1}]
u_*	shear velocity, $(\tau_w/\rho)^{0.5}$ [m s^{-1}]
$\dot{V}$	volume flow rate per tube [m^3 s^{-1}].

Greek symbols

β	spiral angle of the ridge with respect to the tube axis [deg]
Γ	mass rate of condensate flow per unit length [kg m^{-1} s^{-1}]
γ	groove helix angle, $90^\circ - \beta$ [deg]
δ_w	tube wall thickness [m]
μ	dynamic viscosity [Pa s]
ν	kinematic viscosity [m^2 s^{-1}]
ρ	fluid density [kg m^{-3}]
τ	shear stress [Pa].

Dimensionless groups

A_*	reduced tube surface area, A_r/A_s
f	Fanning friction factor, $2\tau_w/(\rho U_m^2)$
$G(e^+, Pr)$	heat transfer roughness function, equation (2)
Nu	Nusselt number, $(h_i D_i/k)$
Pr	Prandtl number, $(c_p\mu/k)$
P_*	reduced pumping power, P_r/P_s
Q_*	increased heat transfer rate, Q_r/Q_s
Re	Reynolds number, $(U_m D_i/\nu)$
$R(e^+)$	momentum transfer roughness function, equation (1)
St	Stanton number, $[h_i/(\rho U_m c_p)]$
W_*	dimensionless mass flow rate, W_r/W_s
β_*	$\beta/90^\circ$
Φ_*	dimensionless group, $(p-t)\cdot s/e^2$.

Subscripts

f	fluid or film
i	inside diameter
m	mean value
o	outside diameter
r	rough tube
s	smooth tube
w	at the wall.

are used to select the most efficient of the tubes and estimate realistically the benefits offered by corrugated tubes for power plant condensers. Possible improvements of the performance of the tubes are also considered.

EXPERIMENTAL PROGRAM

Tube configuration

In the present experimental program 25 spirally corrugated tubes of varying geometries and one standard smooth tube were studied. All tubes had inside diameters of 25.9 mm with wall thicknesses of 1.0 mm before the cold rolling operation. The smooth tube was used for standardizing the experimental set-up and to compare the enhancement in heat transfer and fluid friction. All enhanced tubes were manufactured from smooth tubes with a special fabrication technique which embosses an internal projection, also known as a ridge, in registration with an external groove. This configuration was attained without thinning the tube wall at the focus of the corrugation. Figure 1 shows a sketch of a spirally corrugated tube and the nomenclature used to describe its geometry. The characteristic parameters—pitch of corrugation p, height of corrugation e, spiral angle β, number of spiral starts N, etc.—which define the roughness geometry of the tube, are listed in Table 1(a) and the dimensionless groups in Table 1(b). All characteristics are defined as in refs. [16, 20]. Tubes 11–17 and 21–27 were manufactured in pairs at identical technological conditions but tubes 11–17 were processed by a roll having a radius $r = 1.0$ mm, while tubes 21–27 were processed by a roll with a radius $r = 1.5$ mm.

Experimental work

Figure 2 shows a schematic drawing of the experimental set-up. The actual test section comprised of a 1200 mm long, double pipe heat exchanger, 9, the inner tube of which was either a smooth tube or a

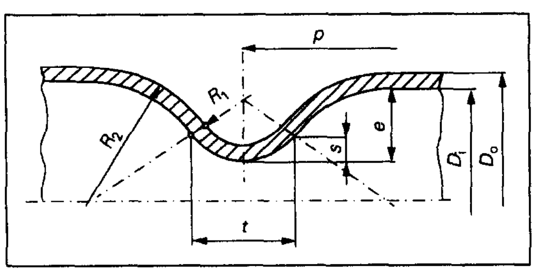

FIG. 1. Characteristic parameters of a corrugated tube.

Table 1(a)

Tube No.	D_o (mm)	D_i (mm)	e (mm)	p (mm)	t (mm)	s (mm)	β (deg)	N starts
11 ○	27.40	25.25	0.808	14.47	2.69	0.327	80.5	1
12 ⦸	27.46	25.43	0.818	14.42	2.77	0.290	80.5	1
13 ⌀	27.27	25.22	0.833	12.41	2.39	0.260	81.8	1
14 ⌽	27.25	25.19	0.805	10.74	2.65	0.300	82.8	1
15 △	27.37	25.31	0.757	10.14	2.60	0.333	83.3	1
16 □	27.40	25.42	0.759	8.64	2.61	0.334	84.3	1
17 ⍁	27.19	25.18	0.984	14.47	2.67	0.388	80.4	1
21 ●	27.20	26.06	0.876	14.46	2.79	0.347	80.4	1
22 ●	27.59	25.44	0.823	14.32	2.87	0.307	80.6	1
23 ●	27.17	25.15	0.869	12.35	2.98	0.390	81.8	1
24 ●	27.10	25.00	0.750	10.64	2.77	0.289	82.9	1
25 ▲	27.43	25.40	0.763	10.05	2.71	0.327	83.3	1
26 ■	27.47	25.34	0.706	8.65	2.46	0.281	84.3	1
27 ■	27.19	25.14	0.972	14.34	3.22	0.446	80.5	1
18 +	27.27	25.20	1.022	10.95	2.65	0.379	82.7	1
19 ×	27.35	25.27	1.071	16.85	3.00	0.487	78.9	1
28 △	27.23	25.26	0.979	10.96	2.91	0.415	82.7	1
29 *	27.50	25.48	1.018	16.85	2.89	0.366	79.0	1
31 ▽	27.33	25.40	0.710	6.49	2.19	0.340	85.7	1
32 ⊖	27.11	24.97	0.943	7.90	2.79	0.463	84.7	1
33 ⊟	27.56	25.62	0.447	6.55	2.18	0.222	85.7	1
34 ⌽	27.62	25.78	0.628	8.48	2.46	0.301	84.4	1
35 ⍂	26.95	24.90	1.165	14.20	2.95	0.463	80.5	1
51 ⌖	27.88	25.77	1.175	10.52	2.19	0.239	70.2	3
52 ⊠	27.59	25.53	0.903	8.63	2.32	0.250	73.4	3

Table 1(b)

N	e/D_i	p/e	β_*	Φ_*	N	e_i/D	p/e	β_*	Φ_*
11	0.032	17.9	0.894	5.90	27	0.039	14.8	0.894	5.25
12	0.032	17.6	0.894	5.05	18	0.041	10.7	0.919	3.01
13	0.035	14.9	0.909	3.75	19	0.042	15.7	0.877	5.88
14	0.032	13.3	0.920	3.75	28	0.039	11.2	0.919	3.49
15	0.030	13.4	0.926	4.38	29	0.040	16.6	0.878	4.93
16	0.030	11.4	0.937	3.50	31	0.028	9.1	0.952	2.90
17	0.039	14.7	0.893	4.73	32	0.038	8.4	0.941	2.66
21	0.034	16.5	0.893	5.28	33	0.017	14.7	0.952	4.86
22	0.032	17.4	0.896	5.19	34	0.024	13.5	0.938	4.59
23	0.035	14.2	0.909	4.84	35	0.047	12.2	0.894	3.84
24	0.030	14.2	0.921	4.04	51	0.046	9.0	0.780	1.44
25	0.030	13.2	0.926	4.12	52	0.035	9.6	0.816	1.93
26	0.028	12.3	0.937	3.49					

spirally corrugated one. The outer tube of the test rig was an iron pipe having an inside diameter of 100 mm. The test tubes were equipped with nine copper–constantan thermocouples of 0.15 mm diameter soldered on the outer surface of the tubes at a distance of 100 mm from each other. The test section was preceded by a smooth tube or spirally corrugated tube calming section 800 mm long, 8, depending on the tube under study. At both the inlet and the outlet, the tube tested was equipped with two measurement stations, each one including four pressure taps set 90 deg apart in a cross-section. The static pressure from the measurement station (the average of tap outputs) was connected to the limbs of a U-tube manometer.

The water was pumped from a reservoir tank, 1, passed through an orifice meter, 4, mixing chamber, 6, smooth, 7, and rough, 8, entrance sections and run through the rough test section followed by another mixing chamber, 11, and cooler, 12. The heat was supplied by condensing steam generated into a boiler, 5, and condensing at vacuum. When the steady state was attained, the flow rate of the test fluid, the tube wall temperatures, inlet and outlet water temperatures and the temperature of the saturated steam were measured. The water flow rate was measured by a calibrated orifice meter and the accuracy of the measurements was estimated at 2% while that of the pressure drop measurements at 5%. The inlet and outlet temperatures of the cooling water were measured by calibrated 0.1°C accurate mercury-in-glass thermometers. The wall temperatures and the temperature of the steam were measured by copper–constantan thermocouples with the same accuracy. The bulk temperature of the water ranged from 54 to 80°C and the corresponding variation of the Prandtl number was 3.4–2.2. All physical properties were evaluated at the aver-

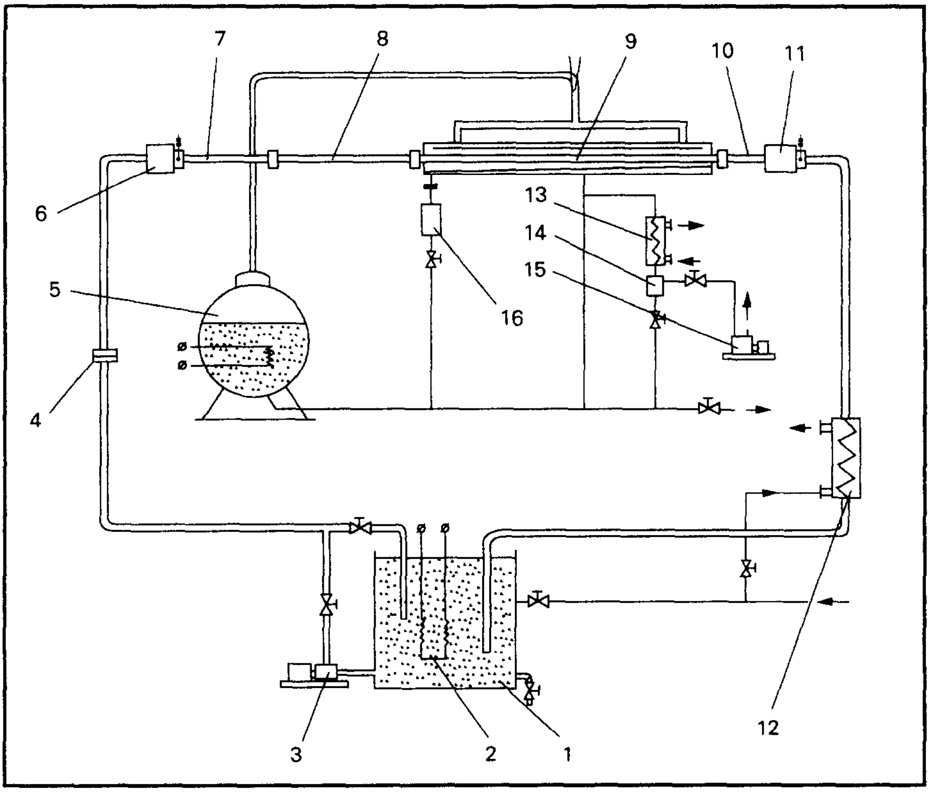

FIG. 2. Schematic diagram of the experimental setup: 1, reservoir; 2, water heater; 3, pump; 4, orifice meter; 5, boiler; 6, calming chamber; 7, smooth entrance section; 8, rough entrance section; 9, rough test section; 10, smooth outlet section; 11, calming chamber; 12, cooler; 13, extra steam condenser; 14, separator; 15, vacuum pump; 16, condensate measuring tank.

age bulk temperature between the inlet and the outlet. The temperature of the steam varied from 60 to 85°C and the corresponding log-mean temperature difference between the steam and the cooling water was 3–7 K.

RESULTS AND DISCUSSION

Fanning friction factors

The isothermal pressure drop studies were conducted at different temperatures of the water in the range from 40 to 80°C in all tubes for turbulent flow of water. Isothermal friction factor coefficients were determined and their uncertainties were estimated at 4%. The friction factor coefficients for the smooth tube were satisfactorily correlated by the Blasius equation

$$f = 0.079Re^{-0.25} \tag{3}$$

over a range of Reynolds numbers from 10^4 to 6×10^4 with a standard deviation of $\pm 3\%$ and this equation was used for calibration of the experimental set-up.

As expected, the turbulent flow friction factors in single- and multistart spirally corrugated tubes were significantly higher than in the smooth tube under the same operating conditions (Fig. 3). A characteristic feature of the flow in spirally corrugated tubes is that even at high flow rates, the friction factor continues to decrease with the increase of *Re* although not so rapidly as in the smooth tube—a behaviour observed earlier [3–12]. Friction factor data were correlated by the following equation:

$$f = c_f Re^m \tag{4}$$

obtained via a curve-fitting procedure. The values of c_f and m were determined for each tube and equation (4) represents the data within $\pm 2\%$ standard deviation. The values for c_f and m are listed in Table 2.

An inspection of Table 1(b) and Fig. 3 indicates that the Fanning friction factors measured for the pairs of tubes 11 and 12; 14 and 24; and 17 and 27 have different values (in pairs) despite the fact that their e/D_i, p/e and β_* are equal. The differences are of the order of 6% for tubes 14 and 24 and 17 and 27 and 16% for tubes 11 and 12. Similar observations were reported in ref. [5] for tubes 1 and 2, where the differences in the friction factor values were about 9%. This fact was observed earlier in ref. [21] for cross groove corrugated tubes where it was pointed out that for equal heights and pitches of the ridges, created

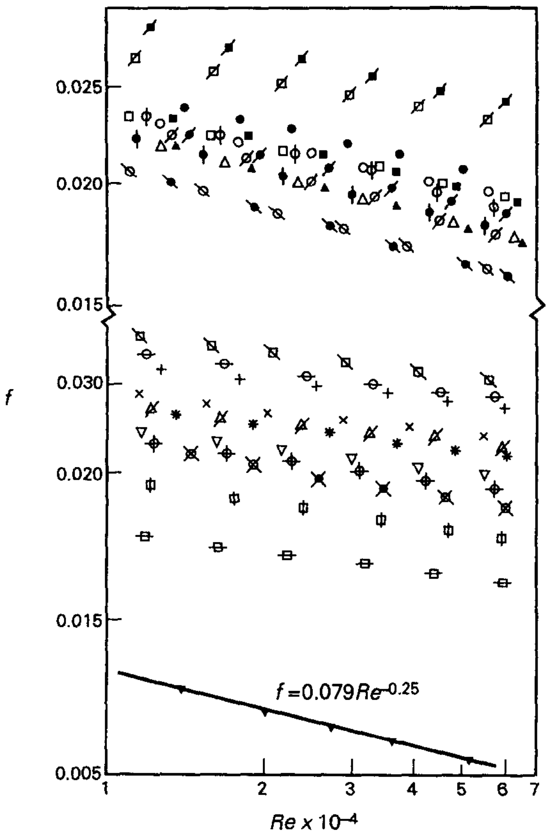

FIG. 3. Friction factor vs Reynolds number.

inside tubes with equal internal diameters, the friction factors could differ by up to 25% according to the technology of the rolling operation. In ref. [22] we discussed the idea that two additional geometrical parameters could be introduced due to their influence on the flow behaviour in the region between two adjacent ridges. The parameters are: t, the axial width of the ridge cap and s, the radial height of the ridge cap. These two parameters are defined as follows: s is the distance between the crest of the ridge and the inflection point where the concave and convex portions of the (symmetric) ridge join each other smoothly and have a common tangent, whereas t is the distance between the inflection points of the two slopes of the ridge. These parameters have been mentioned for the first time in ref. [16] where an attempt has been made to use them in an in-tube heat transfer coefficient correlation but since then they have not appeared in the reports. Similar attempts to introduce the width of the semicircular promoter are encountered in refs. [8, 10].

Having in mind the physical nature of the flow between two adjacent promoters, in ref. [22] we suggest two geometrical complexes to characterize its hydraulic behaviour—$(p-t)/e$ and s/e. The first one characterizes the evolution of the flow separation from the promoter and the second defines the degree of separation of the flow and the swirls after the promoter. Multiplying these two simplexes we introduce a new one

$$\Phi_* = (p-t)\cdot s/e^2$$

to replace the simplex p/e and to take into account the phenomena mentioned above. In ref. [22] we showed that the momentum transfer roughness function $R(e^+)$ could be expressed (on the basis of the experimental results shown on Fig. 3) in the form

$$R(e^+) = 0.416Re^{0.1}(e/D_i)^{-0.42}\beta_*^{-1.94}\Phi_*^{0.08}. \quad (5)$$

Using the correlation, equation (5), the friction factors corresponding to 346 experimental points were calculated. The comparison between experimental and calculated values of f showed a relative difference of more than $\pm 10\%$ for six points only. In ref. [23] we extended this idea and developed a 'mixing-length' model for predicting the friction factor and heat transfer coefficients in spirally corrugated tubes.

Heat transfer

Heat transfer studies in spirally corrugated tubes were carried out to obtain values for the water-side heat transfer coefficients h_i, and the steam condensing coefficients h_o. Since the metal wall temperatures were measured, the individual film heat transfer coefficients were determined from the equation

$$Q = h_oA_o(T_s - T_w)_m = h_iA_i(T_w - T_b)_m \quad (6)$$

where Q is the mean of Q_s (based on the steam condensate measurements) and Q_c (based on the coolant

Table 2

Tube No.	c_f	m	Tube No.	c_f	m	Tube No.	c_f	m
11	0.067	−0.113	21	0.077	−0.122	31	0.082	−0.130
12	0.077	−0.142	22	0.079	−0.145	32	0.120	−0.133
13	0.104	−0.162	23	0.084	−0.137	33	0.052	−0.134
14	0.090	−0.143	24	0.078	−0.134	34	0.089	−0.163
15	0.082	−0.140	25	0.098	−0.157	35	0.139	−0.140
16	0.065	−0.110	26	0.087	−0.138	51	0.081	−0.133
17	0.062	−0.090	27	0.079	−0.108	52	0.141	−0.193
18	0.102	−0.122	28	0.071	−0.104			
19	0.095	−0.128	29	0.093	−0.132			

water). Only those runs for which the heat balance error (HBE), calculated as $[2(Q_s-Q_c)/(Q_s+Q_c)]\cdot 100\%$, was less than $\pm 5\%$ were processed for evaluation of h_i and h_o. The tube wall thermal resistance was accounted for in the calculation of the individual heat transfer coefficients.

Water-side heat transfer coefficient, h_i

The smooth tube heat transfer coefficients were found to agree to within $\pm 3.5\%$ of the Sieder–Tate equation, for turbulent flow heat transfer of water

$$Nu_i = 0.027 Re^{0.8} Pr^{0.33} (\mu_b/\mu_w)^{0.14}. \tag{7}$$

Compared to the Dittus–Boelter equation

$$Nu_i = 0.023 Re^{0.8} Pr^{0.4} \tag{8}$$

the experimental values of h_i were found to be 13% greater than the values calculated from equation (8), thereby suggesting the replacement of 0.023 with 0.026 in equation (8). A similar result was reported in ref. [6] suggesting the value of 0.027. Figure 4 shows the heat transfer data in the form $Nu_i\,Pr^{-0.4}$ as a function of the Reynolds number Re, a counterpart of the friction factor data shown on Fig. 3. Therefore, the heat transfer data were correlated in the form

$$Nu_i\,Pr^{-0.4} = c_h\,Re^n \tag{9}$$

by a curve-fitting procedure and the values of the constants c_h and n, for each tube, are listed in Table 3.

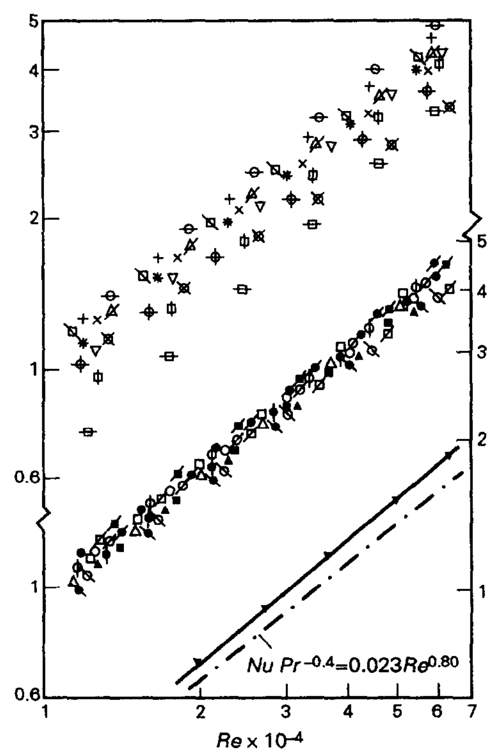

FIG. 4. Water-side heat transfer coefficient vs Reynolds number.

Since many authors [5, 8–11] use the heat transfer roughness function $G(e^+, Pr)$ to analyse their experimental data we calculated the G-function to compare our experimental results with those of other authors. The variation of $G(e^+, Pr)\,Pr^{-0.55}$ with e^+ is shown on Fig. 5. Since the variation of the Prandtl number in our experimental program was in quite narrow limits, $2.15 < Pr < 3.4$, it was not possible to evaluate the Prandtl number effect on the G-function. Consequently we accepted the dependence on Pr in the form $Pr^{0.55}$ as proposed in refs. [8, 10] which agrees well with $Pr^{0.57}$ as reported in ref. [24]. The correlation which fits the experimental points is

$$G(e^+, Pr) = 6.7(e^+)^{0.13}\,Pr^{0.55}. \tag{10}$$

For comparison, the corresponding correlation [10] is also shown on Fig. 5.

Condensation heat transfer coefficient, h_o

Smooth tube condensation heat transfer coefficients obtained from the experiments were compared to those resulting from Nusselt's

$$\frac{h_o}{\left\{\frac{k_f^3\rho_f^2 g}{\mu_f^2}\right\}^{1/3}} = h_o^+ = 1.51(4\Gamma/\mu_f)^{-1/3} \tag{11}$$

where the physical properties are functions of the film temperature calculated as

$$T_f = 0.5(T_s + T_w).$$

The comparison revealed that the heat transfer coefficients calculated from equation (11) underestimate by up to 40% those measured in the experiments. But if one takes into account the fact that generally in the research practice results up to 35% higher than those predicted from equation (11) have been reported, and that the changes of the complex $4\Gamma/\mu_f$ were within quite narrow limits (31.3–39.5) for a more comprehensive estimate, we consider these results acceptable (having also in mind that equation (11) has been derived assuming several simplifications, amongst others a zero steam velocity).

Studying the relationship between performance characteristics and the groove profile, in ref. [25] it has been found convenient to express the corrugated tube results as the ratio (enhancement factor) E_o, defined as

$$E_o = h_{o,r}^+/h_{o,s}^+ \tag{12}$$

where the actual corrugated (roped) surface result is divided by the actual plain surface result at identical conditions. It is well known that the corrugated tube geometry gives rise to surface tension forces and might evoke an enhanced liquid drainage. Following refs. [25, 26] the relationship 'surface tension vs gravity forces' can be expressed as the Weber number We, defined by

Table 3

Tube No.	c_h	n	Tube No.	c_h	n	Tube No.	c_h	n
11	0.075	0.782	21	0.073	0.787	31	0.030	0.871
12	0.050	0.815	22	0.034	0.854	32	0.044	0.848
13	0.047	0.830	23	0.032	0.868	33	0.010	0.945
14	0.047	0.830	24	0.042	0.838	34	0.012	0.950
15	0.034	0.858	25	0.054	0.810	35	0.073	0.792
16	0.035	0.859	26	0.041	0.840	51	0.062	0.790
17	0.115	0.738	27	0.067	0.799	52	0.191	0.673
18	0.060	0.815	28	0.065	0.801			
19	0.112	0.744	29	0.058	0.809	s	0.018	0.835

$$We = \frac{\sigma}{\rho g p}\{1/R_1 + 1/R_2\}. \tag{13}$$

To take into account the fraction of the groove surface, i.e. the groove frequency, we consider the pressure gradient, caused by the surface tension forces, relative to a distance p (one pitch). Using the simple geometry, Fig. 1, the radii R_1 and R_2 can be determined by

$$R_1 = 0.5s[1+0.25(t/s)^2] - \delta_w$$

$$R_2 = 0.5(e-s)\,[1+0.25(t/s)^2] + \delta_w \tag{14}$$

where the geometrical parameters e, t and s have already been used to express the internal friction factors and heat transfer coefficients.

As mentioned in ref. [26] the groove capability to shed condensate at a high rate will obviously depend on the groove helix angle γ. For this reason a simple relation was found by linear regression analysis and the result is shown on Fig. 6. The experimental data could be fitted adequately by the relation

$$E_o = 1.13(We\cos\gamma)^{0.067}. \tag{15}$$

For comparison Catchpole and Drew's relation [26] is given which yields slightly higher values of E_o. This comparison must be considered with a stipulation since the Weber number was defined differently in ref. [26]. Equation (15) confirms the tendency revealed earlier in refs. [12, 26].

Performance evaluation criteria (PEC)

Figures 7–9 represent the criteria FG-2a, FG-3 and VG-1 (FG, fixed geometry; VG, variable geometry) following ref. [19]. The design objectives of these three criteria are:

(i) Case FG-2a—to maximize the heat transfer rate for equal pumping power and heat exchange surface area ($P_* = A_* = 1$). This criterion involves a direct replacement of smooth tubes by augmented tubes of equal length typical for the power plant condenser retubing. The pumping power is maintained constant by reducing the tube-side velocity and thus the exchanger flow rate.

(ii) Case FG-3—to minimize the pumping power for equal heat duty and surface area ($Q_* = A_* = 1$).

(iii) Case VG-1—to reduce the tube surface area for equal pumping power and heat duty ($P_* = Q_* = 1$). In this case the exchanger flow rate is held constant and it is necessary to increase the flow frontal area to satisfy the pumping power constraint.

The performance characteristics of the tubes

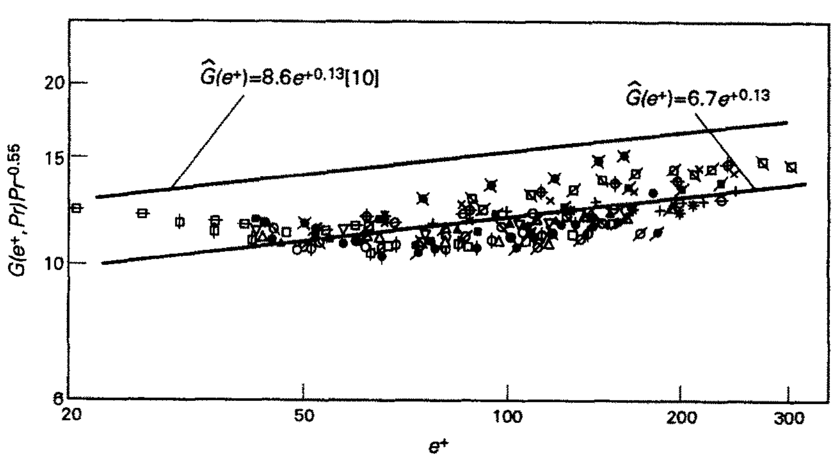

FIG. 5. Variation of $G(e^+, Pr)Pr^{-0.55}$ with roughness Reynolds number, e^+.

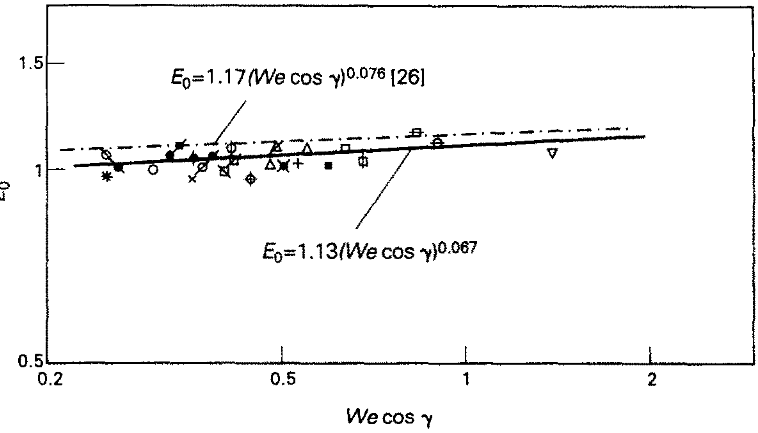

FIG. 6. Steam-side enhancement factor vs $We \cos \gamma$.

studied, shown in Figs. 7–9, were obtained taking into account the thermal resistance across the metal tube wall, enhancement on the outer tube surfaces ($E_o \neq 1$) and the tube-side fouling resistance (which was assumed zero in the preliminary calculations).

It is well known [19] that the FG cases operate at reduced exchanger flow rate ($W_* < 1$) which penalizes the augmented exchanger whereas such a penalty does not occur for the VG cases, which maintain $W_* = 1$. Nevertheless, tubes 16 and 28 show an increase in the heat transfer duty of 25–30% in the range of Reynolds numbers studied. Tube 34 also deserves attention since for $Re > 3.5 \times 10^4$ it shows the best performance (Fig. 7). When the objective is to reduce the surface area with specified flow rate (case VG-1, Fig. 9) tubes 32, 14, 16 and 28 show a reduction of surface area of 38–48% in the range of Reynolds numbers studied.

Water-side fouling is well known as a major contributor to poor condenser performance. Figure 10(a) shows its effect on the increased heat transfer rate (case FG-2a) for tubes 16 and 34. When the tube-side fouling resistance is 5.8×10^{-5} m^2 K W^{-1} (conventionally used in the condenser design), it causes a penalty for the performance ratio of 4–9% in the

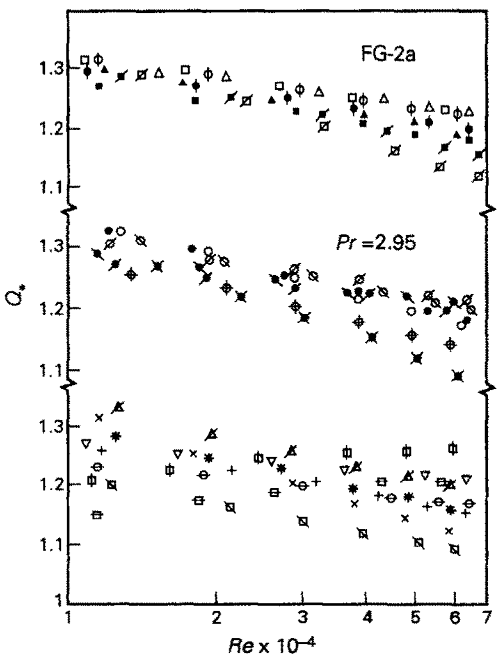

FIG. 7. Increased heat transfer rate for equal pumping power and heat transfer surface vs Reynolds number.

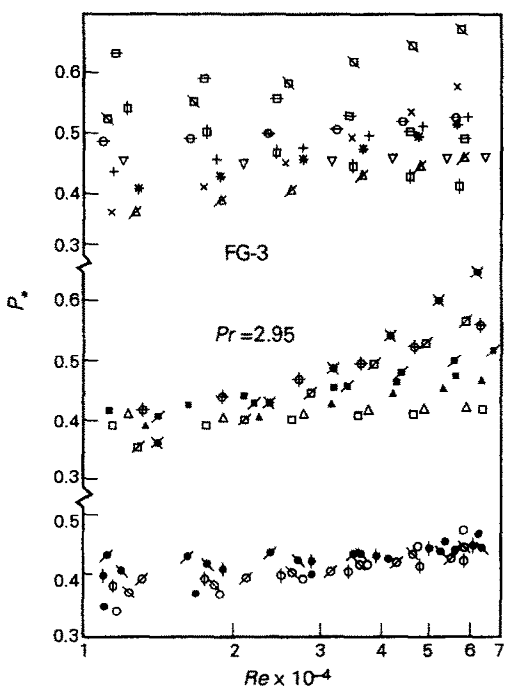

FIG. 8. Reduced pumping power for equal heat duty and heat transfer surface vs Reynolds number.

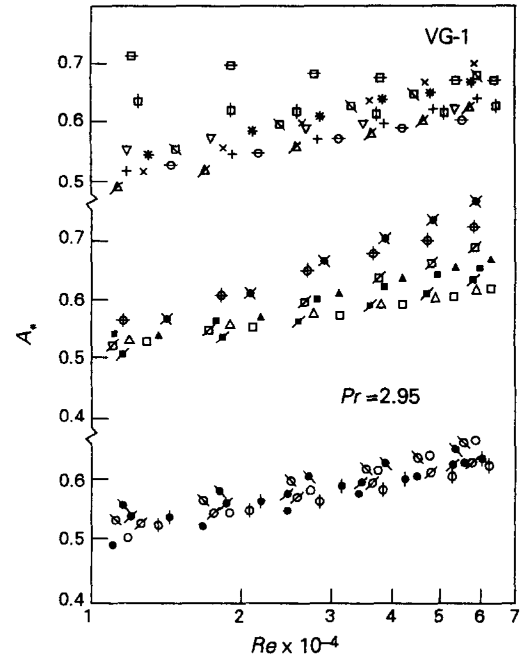

FIG. 9. Reduced heat transfer surface for equal pumping power and heat duty vs Reynolds number.

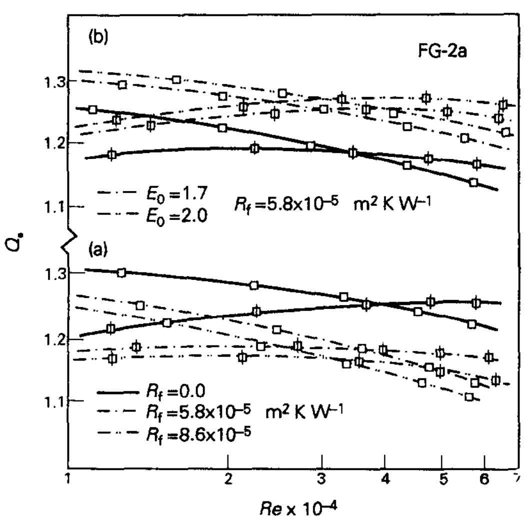

FIG. 10. Increased heat transfer rate for equal pumping power and heat transfer surface vs Reynolds number.

range of Reynolds numbers studied. The importance that the corrugated tubes be kept clean is evident. A possibility to improve the performance of the tube is if an additional external enhancement is being applied, such as in the case of the tubes manufactured by IMI Yorkshire Alloys, Ltd., Leeds [12]. Tubes 16 and 34 have an external enhancement factor $E_o = 1.12$ and 1.07, respectively. If their external enhancement factors are improved up to the value of 1.7 (enhancement factor of the tubes manufactured in ref. [12]) this would increase their performance ratios by 4–7% even though a water-side fouling resistance of 5.8×10^{-5} m^2 K W^{-1} is available (Fig. 10(b)). This, however, requires a different configuration of the tube geometry on each side of the tube.

It should be emphasized that the performance of the tubes evaluated on the basis of these criteria do not include the effects of the vapour shear, condensate inundation and non-condensible gas concentration which might also influence the final selection of the tubes for use in power plant condensers.

CONCLUSIONS

The results of the present study can be summarized as follows:

(1) All spirally corrugated tubes showed an internal enhancement factor ranging from 1.77 to 2.73 and an external enhancement factor from 0.99 to 1.22. An increase of the friction factor coefficient from 100 to 400%, compared to the smooth tube, was observed.

(2) A correlation for the momentum transfer roughness function $R = R(Re, e/D_i, \beta_*, \Phi_*)$ based on the results of the present work was derived including additional geometrical parameters of the ridge. A correlation for the heat transfer roughness function $G(e^+, Pr)$ was also proposed to enable the comparison with other heat transfer data and the prediction of internal heat transfer augmentation published elsewhere. A simple correlation for the external heat transfer enhancement factor was also obtained, including the additional geometrical parameters of the ridge, to complete the mathematical model.

(3) Performance evaluation criteria were used to assess the benefits of replacing the smooth tubes in power plant condensers with corrugated ones. An increase of the heat transfer rate up to 25% and more can be achieved. The reduction or elimination of the tube fouling will also improve the thermal efficiency of the condenser.

Acknowledgements—The authors feel indebted to Prof. A. E. Bergles, Iowa State University and Prof. R. L. Webb, Pennsylvania State University, for supplying them with refs. [1, 2]. We are very grateful to Mr G. Wildsmith and Dr K. T. Jackson from IMI Yorkshire Alloys Ltd., Leeds, and Dr D. L. Pearce from CERL, Leatherhead, U.K., for the many stimulating discussions on the manufacture and performance characteristics of the corrugated (roped) tubes and some quite useful references.

REFERENCES

1. A. E. Bergles, R. L. Webb, G. H. Junkhan and M. K. Jensen, Bibliography on augmentation of convective heat and mass transfer, Report No. HTL-19, Engineering Research Institute, Iowa State University (1979).
2. R. L. Webb, A. E. Bergles and G. H. Junkhan, Bibliography of U.S. patent literature on heat transfer augmentation techniques, Report No. HTL-25, Engineering Research Institute, Iowa State University (1980).

3. J. G. Withers and E. H. Young, Steam condensing on vertical rows of horizontal corrugated and plain tubes, *Ind. Engng Chem. Process Des. Dev.* **10**(1), 19–30 (1971).
4. E. H. Young, J. G. Withers and W. B. Lampert, Heat transfer characteristics of corrugated tubes in steam condensing applications, *A.I.Ch.E. Symp. Ser.* **74**(174), 15–24 (1978).
5. J. G. Withers, Tube-side heat transfer and pressure drop for tubes having helical internal ridging with turbulent/transitional flow of single-phase fluid. Part I. Single-helix ridging, *Heat Transfer Engng* **2**(1), 48–58 (1980).
6. M. H. Mehta and M. Raja Rao, Heat transfer and frictional characteristics of spirally enhanced tubes for horizontal condensers. In *Advances of Enhanced Heat Transfer*, pp. 11–21. ASME, New York (1979).
7. P. J. Marto, D. J. Reilly and J. H. Fenner, An experimental comparison of enhanced heat transfer condensing tubing. In *Advances in Enhanced Heat Transfer*, pp. 1–10. ASME, New York (1979).
8. S. Ganeshan and M. Raja Rao, Studies on thermohydraulics of single and multistart spirally corrugated tubes for water and time independent power law fluids, *Int. J. Heat Mass Transfer* **25**, 1013–1022 (1982).
9. W. Nakayama, K. Takahashi and T. Daikoku, Spiral ribbing to enhance single-phase heat transfer inside tubes, *ASME/JSME Thermal Engng Joint Conf. Proc.*, Honolulu, Hawaii, Vol. 1, pp. 365–372 (1983).
10. R. Sethumadhavan and M. Raja Rao, Turbulent flow friction and heat transfer characteristics of single- and multistart spirally enhanced tubes, *Trans. ASME*, Ser. C, *J. Heat Transfer* **108**, 55–61 (1986).
11. H. M. Li, K. S. Ye, Y. K. Tan and S. J. Deng, Investigation on tube side flow visualization, friction and heat transfer characteristics of helical ridging tubes, *Proc. 7th Int. Heat Transfer Conf.*, Münich, Vol. 3, pp. 75–80 (1982).
12. Anon., YIA heat exchanger tubes: design data for horizontal roped tubes in steam condensers, Technical Memorandum 3, Yorkshire Imperial Alloys, Leeds, U.K. (1976).
13. L. D. Berman, A. K. Kirsh and G. M. Konovalov, Spirally corrugated tubes utilized in power station condensers, *Thermoenergy* **1**, 46–50 (1984) (in Russian).
14. M. Rowe, Power plant condensers—recent CEGB experience, *Int. Chem. Engng Symp. Ser.* No. 75, 113–134 (1983).
15. L. W. Boyd, J. C. Hammon, J. J. Litterell and J. G. Withers, Efficiency improvement at Gallatin Unit 1 with corrugated condenser tubing, Joint Power Generation Conf., Paper No. 83-JPGC-Pwr-4 (1983).
16. J. G. Withers, E. P. Hardas and M. W. Jurmo, Internally ridged heat transfer tube and method of designing for optimum performance, U.S. Patent No. 3779312 (1973).
17. A. E. Bergles, A. R. Blumenkrantz and J. Taborek, Performance evaluation criteria for enhanced heat transfer surfaces, *5th Int. Heat Transfer Conf.*, Tokyo, Vol. 2, pp. 239–243 (1974).
18. A. E. Bergles, R. L. Bunn and G. H. Junkhan, Extended performance evaluation criteria for enhanced heat transfer surfaces, *Lett. Heat Mass Transfer* **1**, 113–120 (1974).
19. R. L. Webb, Performance evaluation criteria for use of enhanced heat transfer surfaces in heat exchanger design, *Int. J. Heat Mass Transfer* **24**, 715–726 (1981).
20. W. J. Marner, A. E. Bergles and J. M. Chenoweth, On the presentation of performance data for enhanced tubes used in shell-and-tube heat exchangers, *Trans. ASME*, Ser. C, *J. Heat Transfer* **105**, 358–365 (1983).
21. E. K. Kalinin, G. A. Dreitser and S. A. Yarkho, *Heat Transfer Intensification in Channels*. Mashinostroenie, Moscow (1972) (in Russian).
22. V. D. Zimparov and N. L. Vulchanov, Turbulent hydraulic friction in spirally corrugated tubes for condenser applications, *Theor. Appl. Mech.* **XXI**(2), 56–61 (1990).
23. N. L. Vulchanov, V. D. Zimparov and L. B. Delov, Heat transfer and friction characteristics of spirally corrugated tubes for power plant condensers—2. A 'mixing-length' model for predicting fluid friction and heat transfer, *Int. J. Heat Mass Transfer* **34**, 2199–2206 (1991).
24. R. L. Webb, E. R. G. Eckert and R. J. Goldstein, Heat transfer and friction in tubes with repeated-rib roughness, *Int. J. Heat Mass Transfer* **14**, 601–617 (1971).
25. V. D. Zimparov and N. L. Vulchanov, Condensation of steam on corrugated (roped) tubes for horizontal condensers—the heat transfer coefficient, *Theor. Appl. Mech.* (in press).
26. J. P. Catchpole and B. C. H. Drew, Evaluation of some shaped tubes for steam condensers, Steam Turbine Condensers, Report of a Meeting at NEL, 17–18 September 1974, East Kilbride, Glasgow, U.K., pp. 68–75 (1974).

CARACTERISTIQUES DE TRANSFERT THERMIQUE ET DE FROTTEMENT POUR DES TUBES CORRUGUES EN SPIRALE POUR CONDENSEURS DE CENTRALE THERMIQUE—I. ETUDE EXPERIMENTALE ET EVALUATION DES PERFORMANCES

Résumé—Des résultats sur le transfert thermique et la perte de pression par frottement isotherme sont obtenus expérimentalement pour un tube lisse et 25 tubes en cuivre corrugués en spirale afin d'application à un condenseur de centrale thermique. La hauteur d'arête varie entre 0,44 et 1,18 mm et le pas de corrugation de 6,5 à 16,9 mm. L'angle de la spirale (par rapport à l'axe du tube) est dans la plage 68–85 degrés et le nombre de Reynolds entre 10^4 et 6×10^4. Le transfert thermique et la perte de pression sont sous une forme favorable à une comparaison facile avec les données des autres auteurs. On peut prédire théoriquemnent le facteur de frottement et l'accroissement de transfer thermique des deux côtés du tube à l'aide d'un modèle mathématique dans lequel on entre les nombres de Reynolds et de Prandtl ainsi que les paramètres géométriques. Des critères d'évaluation de performance sont utilisés pour obtenir des estimations quantitatives des bénéfices permis par les tubes corrugués en spirale.

WÄRMEÜBERGANG UND DRUCKABFALL AN SPIRALFÖRMIG GERILLTEN ROHREN FÜR KRAFTWERKSKONDENSATOREN—1. EXPERIMENTELLE UNTERSUCHUNG

Zusammenfassung—Es wird der Wärmeübergang und der isotherme Druckabfall für ein glattes und 25 spriralförmig gerillte Messingrohre, wie sie für Kraftwerkskondensatoren verwendet werden, experimentell ermittelt. Die Rillenhöhe wird von 0,44 bis 1,18 mm, der Rillenabstand von 6,5 bis 16,9 mm variiert. Der Spiralwinkel der Rille (bezogen auf die Rohrachse) liegt im Bereich zwischen 68° und 85°, die Reynolds-Zahl zwischen 10^4 und 6×10^4. Die Ergebnisse für Wärmeübergang und Druckabfall werden so dargestellt, daß sie einfach mit den Ergebnissen anderer Autoren verglichen werden können. Die Ergebnisse werden dann dazu verwendet, den Reibungsbeiwert und die Verbesserung des Wärmeübergangs an beiden Rohrseiten mit Hilfe eines vereinheitlichten Modells zu berechnen, das als Eingabegrößen die Reynolds- und die Prandtl-Zahl sowie die Geometrie der Rille benötigt. Es werden Kriterien zur Leistungsbestimmung verwendet, um die Vorteile spiralförmig gerillter Rohre quantitativ abzuschätzen.

ХАРАКТЕРИСТИКИ ТЕПЛОПЕРЕНОСА И ТРЕНИЯ ТРУБ СО СПИРАЛЬНЫМ ОРЕБРЕНИЕМ В КОНДЕНСАТОРАХ ЭНЕРГЕТИЧЕСКИХ УСТАНОВОК—1. ЭКСПЕРИМЕНТАЛЬНОЕ ИССЛЕДОВАНИЕ И ОЦЕНКА РАБОЧИХ ХАРАКТЕРИСТИК

Аннотация—Получены экспериментальные данные по теплопереносу и перепаду давления за счет трения в изотермическом случае для одной гладкой и 25 труб со спиральным оребрением из латуни, используемых в конденсаторах энергетических установок. Высота ребер изменялась от 0,44 до 1,18 мм, а шаг между ними—от 6,5 до 16,9 мм. Диапазон изменения числа Рейнольдса составлял 10^4–6×10^4, а угол наклона ребра относительно оси трубы—68–85°. Данные по теплопереносу и перепаду давления представлены в виде, удобном для сравнения с результатами других авторов. Они используются для теоретического расчета коэффициентов трения и интенсификации теплопереноса по обе стороны трубы с помощью обобщенной математической модели, для которой требуется знание чисел Рейнольдса и Прандтля на входе, а также геометрических параметров ребра. На основе определения рабочих характеристик получены количественные оценки преимуществ труб со спиральным оребрением.